Widely-tunable mid-infrared fiber-coupled quartz-enhanced photoacoustic sensor for environmental monitoring

M. Siciliani de Cumis,[1] S. Viciani,[1] S. Borri,[1,*] P. Patimisco,[2] A. Sampaolo,[2] G. Scamarcio,[2] P. De Natale,[1] F. D'Amato,[1] and V. Spagnolo[2]

[1] *CNR - Istituto Nazionale di Ottica (INO) and European Laboratory for Nonlinear Spectroscopy (LENS), Via Carrara 1, 50019 Sesto Fiorentino FI, Italy*

[2] *Dipartimento Interateneo di Fisica, Università degli Studi di Bari, Politecnico di Bari and CNR - Istituto di Fotonica e Nanotecnologie (IFN) UOS Bari, via Amendola 173, 70126 Bari BA, Italy*

[*] *simone.borri@ino.it*

Abstract: A compact widely-tunable fiber-coupled sensor for trace gas detection of hydrogen sulfide (H_2S) in the mid infrared is reported. The sensor is based on an external-cavity quantum cascade laser (EC-QCL) tunable between 7.6 and 8.3 μm wavelengths coupled into a single-mode hollow-core waveguide. Quartz-enhanced photoacoustic spectroscopy has been selected as detecting technique. The fiber coupling system converts the astigmatic beam exiting the laser into a TEM_{00} mode. During a full laser scan, we observed no misalignment between the optical beam and the tuning fork, thus making our system applicable for multi-gas or broad absorber detections. The sensor has been tested on N_2:H_2S gas mixtures. The minimum detectable H_2S concentration is 450 ppb in ~3 s integration time, which is the best value till now reported in literature for H_2S optical sensors.

OCIS codes: (280.3420) Laser sensors; (120.6200) Spectrometers and spectroscopic instrumentation; (140.5965) Semiconductor lasers, quantum cascade; (060.2390) Fiber optics, infrared.

References and links

1. A. A. Kosterev, Y. A. Bakhirkin, R. F. Curl, and F. K. Tittel, "Quartz-enhanced photoacoustic spectroscopy," Opt. Lett. **27**(21), 1902–1904 (2002).
2. A. A. Kosterev, F. K. Tittel, D. V. Serebryakov, A. L. Malinovsky, and I. V. Morozov, "Applications of quartz tuning forks in spectroscopic gas sensing," Rev. Sci. Instrum. **76**(4), 043105 (2005).
3. G. Gagliardi, F. Tamassia, P. De Natale, C. Gmachl, F. Capasso, D. L. Sivco, J. N. Baillargeon, A. L. Hutchinson, and A. Y. Cho, "Sensitive detection of methane and nitrous oxide isotopomers using a continuous wave quantum cascade laser," Eur. Phys. J. D **19**(3), 327–331 (2002).
4. A. Hugi, R. Maulini, and J. Faist, "External cavity quantum cascade laser," Semicond. Sci. Technol. **25**(8), 083001 (2010).
5. M. Razeghi, "High-Performance InP-Based Mid-IR Quantum Cascade Lasers," IEEE J. Sel. Top. Quantum Electron. **15**(3), 941–951 (2009).
6. P. Patimisco, G. Scamarcio, F. K. Tittel, and V. Spagnolo, "Quartz-Enhanced Photoacoustic Spectroscopy: A Review," Sensors (Basel) **14**(4), 6165–6206 (2014).
7. A. A. Kosterev, F. K. Tittel, D. V. Serebryakov, A. L. Malinovsky, and I. V. Morozov, "Applications of quartz tuning forks in spectroscopic gas sensing," Rev. Sci. Instrum. **76**(4), 043105 (2005).
8. L. Dong, A. A. Kosterev, D. Thomazy, and F. K. Tittel, "QEPAS spectrophones: design, optimization, and performance," Appl. Phys. B **100**(3), 627–635 (2010).
9. K. Liu, H. Yi, A. A. Kosterev, W. Chen, L. Dong, L. Wang, T. Tan, W. Zhang, F. K. Tittel, and X. Gao, "Trace gas detection based on off-beam quartz enhanced photoacoustic spectroscopy: Optimization and performance evaluation," Rev. Sci. Instrum. **81**(10), 103103 (2010).
10. L. Dong, V. Spagnolo, R. Lewicki, and F. K. Tittel, "Ppb-level detection of nitric oxide using an external cavity quantum cascade laser based QEPAS sensor," Opt. Express **19**(24), 24037–24045 (2011).

#217183 - $15.00 USD Received 16 Jul 2014; revised 15 Sep 2014; accepted 15 Sep 2014; published 5 Nov 2014

11. V. Spagnolo, P. Patimisco, S. Borri, G. Scamarcio, B. E. Bernacki, and J. Kriesel, "Part-per-trillion level SF_6 detection using a quartz enhanced photoacoustic spectroscopy-based sensor with single-mode fiber-coupled quantum cascade laser excitation," Opt. Lett. **37**(21), 4461–4463 (2012).
12. J. Hodgkinson and R. P. Tatam, "Optical gas sensing: a review," Meas. Sci. Technol. **24**(1), 012004 (2013).
13. S. Borri, P. Patimisco, I. Galli, D. Mazzotti, G. Giusfredi, N. Akikusa, M. Yamanishi, G. Scamarcio, P. De Natale, and V. Spagnolo, "Intracavity quartz-enhanced photoacoustic sensor," Appl. Phys. Lett. **104**(9), 091114 (2014).
14. S. Borri, P. Patimisco, A. Sampaolo, M. S. Vitiello, H. E. Beere, D. A. Ritchie, G. Scamarcio, and V. Spagnolo, "Terahertz quartz enhanced photo-acoustic sensor," Appl. Phys. Lett. **103**(2), 021105 (2013).
15. P. Patimisco, S. Borri, A. Sampaolo, H. E. Beere, D. A. Ritchie, M. S. Vitiello, G. Scamarcio, and V. Spagnolo, "A quartz enhanced photo-acoustic gas sensor based on a custom tuning fork and a terahertz quantum cascade laser," Analyst (Lond.) **139**(9), 2079–2087 (2014).
16. V. Spagnolo, A. A. Kosterev, L. Dong, R. Lewicki, and F. K. Tittel, "NO trace gas sensor based on quartz enhanced photoacoustic spectroscopy and external cavity quantum cascade laser," Appl. Phys. B **100**(1), 125–130 (2010).
17. G. Wysocki, R. Lewicki, R. F. Curl, F. K. Tittel, L. Diehl, F. Capasso, M. Troccoli, G. Hofler, D. Bour, S. Corzine, R. Maulini, M. Giovannini, and J. Faist, "Widely tunable mode-hop free external cavity quantum cascade lasers for high resolution spectroscopy and chemical sensing," Appl. Phys. B **92**(3), 305–311 (2008).
18. http://www.irflex.com/news/new-singlemode-mid-ir-fibers-have-been-added-existing-irf-s-series-chalcogenide-nonlinear-mid
19. C. M. Bledt, J. A. Harrington, and J. M. Kriesel, "Loss and modal properties of Ag/AgI hollow glass waveguides," Appl. Opt. **51**(16), 3114–3119 (2012).
20. V. Spagnolo, P. Patimisco, S. Borri, G. Scamarcio, B. E. Bernacki, and J. Kriesel, "Mid-infrared fiber-coupled QCL-QEPAS sensor," Appl. Phys. B **112**(1), 25–33 (2013).
21. J. M. Kriesel, G. M. Hagglund, N. Gat, V. Spagnolo, and P. Patimisco, "Spatial mode filtering of mid-infrared (mid-IR) laser beams with hollow core fiber optics", Proc. SPIE 8993, Quantum Sensing and Nanophotonic Devices **XI**, 89930V (2013).
22. U. Willer, D. Scheel, I. Kostjucenko, C. Bohling, W. Schade, and E. Faber, "Fiber-optic evanescent-field laser sensor for in-situ gas diagnostics," Spectrochim. Acta A Mol. Biomol. Spectrosc. **58**(11), 2427–2432 (2002).
23. W. Chen, A. A. Kosterev, F. K. Tittel, X. Gao, and W. Zhao, "H_2S trace concentration measurements using off-axis integrated cavity output spectroscopy in the near-infrared," Appl. Phys. B **90**(2), 311–315 (2008).
24. A. A. Kosterev, L. Dong, D. Thomazy, F. K. Tittel, and S. Overby, "QEPAS for chemical analysis of multi-component gas mixtures," Appl. Phys. B **101**(3), 649–659 (2010).
25. A. Varga, Z. Bozóki, M. Szakáll, and G. Szabó, "Photoacoustic system for on-line process monitoring of hydrogen sulfide (H_2S) concentration in natural gas streams," Appl. Phys. B **85**(2-3), 315–321 (2006).
26. J. A. Harrington, "Infrared Fibers and Their Applications," SPIE Press, Bellingham, WA (2004).
27. R. Nubling and J. A. Harrington, "Launch conditions and mode coupling in hollow glass waveguides," Opt. Eng. **37**(9), 2454–2458 (1998).
28. P. Patimisco, V. Spagnolo, M. S. Vitiello, G. Scamarcio, C. M. Bledt, and J. A. Harrington, "Low-loss hollow waveguide fibers for mid-infrared quantum cascade laser sensing applications," Sensors (Basel) **13**(1), 1329–1340 (2013).
29. L. S. Rothman, I. E. Gordon, Y. Babikov, A. Barbe, D. Chris Benner, P. F. Bernath, M. Birk, L. Bizzocchi, V. Boudon, L. R. Brown, A. Campargue, K. Chance, E. A. Cohen, L. H. Coudert, V. M. Devi, B. J. Drouin, A. Fayt, J. M. Flaud, R. R. Gamache, J. J. Harrison, J. M. Hartmann, C. Hill, J. T. Hodges, D. Jacquemart, A. Jolly, J. Lamouroux, R. J. Le Roy, G. Li, D. A. Long, O. M. Lyulin, C. J. Mackie, S. T. Massie, S. Mikhailenko, H. S. P. Müller, O. V. Naumenko, A. V. Nikitin, J. Orphal, V. Perevalov, A. Perrin, E. R. Polovtseva, C. Richard, M. A. H. Smith, E. Starikova, K. Sung, S. Tashkun, J. Tennyson, G. C. Toon, V. G. Tyuterev, and G. Wagner, "The HITRAN 2012 molecular spectroscopic database," J. Quant. Spectrosc. Radiat. Transf. **130**, 4–50 (2013).
30. H.-J. Bauer, A. C. C. Paphitis, and R. Schotter, "Vibrational and rotational relaxation in Hydrogen Sulfide," Physica **47**(1), 109–112 (1970).

1. Introduction

Environmental monitoring is among the topics of larger interest for both scientific and civil purposes. Real-time in situ monitoring of toxic emissions in industrial environments is one of the main issues and requires robust, compact and sufficiently performing sensors. Efficient detection can be pursued essentially by following two approaches: selection of a high-sensitivity spectroscopic technique and choice of the most suitable absorption range. The latter has to take into account the presence of interference absorption effects by molecules such as H_2O or CO_2, due to their high concentration level in ambient air, as well as the availability of suitable instrumentation such as sufficiently high power laser sources and sensitive detectors.

#217183 - $15.00 USD Received 16 Jul 2014; revised 15 Sep 2014; accepted 15 Sep 2014; published 5 Nov 2014

Since its first demonstration in 2002 [1], quartz-enhanced photoacoustic spectroscopy (QEPAS) has earned a place among the high-sensitivity spectroscopic techniques, particularly suited for in-field application. It allows for compact and robust apparatus, with a much simpler optical configuration with respect to competitive techniques such as cavity ring down (CRD) spectroscopy or integrated cavity output (ICOS) spectroscopy and thus requires much simpler alignment procedures. QEPAS is an alternative approach to standard photoacoustic detection of trace gas utilizing a quartz tuning fork (QTF) as a sharply resonant acoustic transducer to detect weak photoacoustic excitation and allowing the use of extremely small volumes [1,2]. Such an approach removes restrictions imposed on the gas cell by the acoustic resonance conditions. Piezoelectric QTFs, which are typically employed as a frequency standard in clocks, watches and smart phones are used as photoacoustic transducers. They are characterized by a resonant frequency of 2^{15} or ~32,768 Hz and possess a Q ≈100,000 or higher when encapsulated in vacuum and a Q ≈10,000 at normal atmospheric pressure. From the acoustical point of view QTF is a quadrupole, which provides good environmental noise immunity.

The recent development and commercialization of quantum cascade lasers (QCLs) have a strong impact in the field of trace-gas detection for environmental monitoring [3], as they gather, in a compact laser source, useful features like robustness, wavelength agility, high emission power [4,5]. Very efficient mid-IR QCL-based QEPAS sensors have been demonstrated for trace detection of several chemical species, such as NH_3, NO, CO_2, N_2O, CO, CH_2O, C_3H_6O, etc [6–10]. A record detection limit of 50 parts per trillion has been reported for SF_6 [11], corresponding to a normalized noise equivalent absorption (NNEA) value of $2.7 \cdot 10^{-10}$ $W \cdot cm^{-1} \cdot Hz^{-1/2}$, comparable with the best values obtained using highly sensitive techniques, such as CRD and ICOS, characterized by very long optical path lengths [12]. Moreover, one of the main advantages of the QEPAS is that optical detectors are not needed. Recently, a sensor combining QEPAS with high finesse optical cavities (Intracavity-QEPAS) has been demonstrated, leading to possible improved sensitivity of more than two orders of magnitude higher with respect to standard QEPAS apparatuses [13]. A QCL-based QEPAS sensor operating in the THz [14,15] range has been also developed, with detection capabilities at the same levels of the best reported for mid-IR ones.

To further enhance the QEPAS signal, a so-called micro-resonator (mR) can be added to the QTF. The mR consists of two thin metallic or glass tubes. The QTF is positioned between the tubes to probe the acoustic wave excited in the gas contained inside the mR. It is mandatory that the laser radiation passes through the acoustic detection module (ADM) composed by the mR and QTF without hitting it, otherwise the radiation absorbed or blocked by mR or QTF results in a undesirable non-zero background. This signal is usually several times larger than the thermal noise level of QEPAS and carries a shifting fringe-like interference pattern, which strongly limits the QEPAS detection limit [8,16].

The use of mid-IR external cavity (EC)-QCLs, able to cover with a single-device a tuning range larger than 100 cm^{-1}, enables the QEPAS sensor to monitor a large number of different molecules by proper tuning of the laser frequency [17]. The accuracy of this multi-gas sensing depends on the capability of keeping the laser focused between the prongs of the ADM during the spectral scan. In fact, wide EC-QCL tuning is achieved by rotating the first order diffraction coupled back into the QCL, forming the external cavity. This mechanical operation leads to small variations of the laser beam shape and output direction. Due to strict requirements on beam focusing between the ADM, alignment re-optimization is required, unless some strategies are adopted. A suitable approach can be the use of single-mode fiber-coupled systems to deliver the radiation from the laser to the QEPAS module. Indeed, the fiber may force the laser beam into a TEM_{00}-like mode and preserve the optical alignment with the QTF detection system.

Only very recently, low-loss single-mode fibers have become commercially available in the mid-IR range. Solid-core chalcogenide glass fibers operate in single-mode in the range

#217183 - $15.00 USD Received 16 Jul 2014; revised 15 Sep 2014; accepted 15 Sep 2014; published 5 Nov 2014

1.5-6 μm, since for longer wavelengths these fibers attenuate strongly, due to absorption from chalcogenide glass at the edge of the fiber core [18]. Hollow core waveguides (HWG) with bore diameters as large as 30 times the wavelength have been shown to provide a convenient, relatively low-loss means of delivering mid-IR beams with a single spatial mode. Up to now, HWG with bore size down to 200 μm and operating in single mode in the range 5-11 μm, have been demonstrated [19–21].

We report here on a QEPAS sensor based on a HWG coupled with an EC-QCL operating in the range 7.6-8.3 μm. In this work, we use a single-mode HWG with inner silver–silver iodine (Ag–AgI) coatings and internal core diameter of 200 μm. To our knowledge, this is the first time that a single mode fiber has been used in this spectral range for sensing applications. A detailed analysis of the optical performances of the employed HWG as a function of the optical coupling configuration allows us to identify the best operating condition in terms of waveguide losses and single mode beam profile at the waveguide exit. The final output focuser has been designed to provide a beam size and waist small enough to be focused through the mR and between the QTF prongs without hitting them.The sensor has been tested on hydrogen sulfide (H_2S), a molecule of high interest for environmental monitoring due to its high toxicity.

Several sensors for H_2S detection using DFB lasers operating around 1.57 μm have been reported [22–25]. The best results were obtained with off-axis integrated cavity output spectroscopy (OA-ICOS), leading to a minimum detectable concentration of 670 ppm for a 3 s averaging time [23], and 500 ppb detection limit was achieved with a dual-channel H_2S photoacoustic sensor [25]. With our mid-IR QEPAS system we reached a H_2S detection limit in both dry and wet N_2 down to 450 ppb in 3 seconds integration time (330 ppb for 30s integration time), which represents the best achieved value with optical techniques.

2. Experimental setup

For our QEPAS sensor we selected a room-temperature continuous-wave EC-QCL (Daylight Solutions CW-Pulsed) emitting from 1205 to 1310 cm^{-1} (7.6 to 8.3 μm wavelength) as laser source, with an output power up to 90 mW and wavelegth accuracy ± 1.5 cm^{-1}. The latter feature is not a problem if broad absorption lines are investigated (like those of dioxins, for example), but becomes critical when dealing with gas samples, even at atmospheric pressure. Mode-hop free EC-QCLs have a wavelength setting precision down to 0.01 cm^{-1} but, as this is not the case, in order to achieve higher resolution than 1 wavenumber, fine tuning can be obtained by changing the laser temperature. A specific Labview program was written in order to precisely control the laser temperature via the internal Peltier element, allowing for fine spectral scans of several GHz (tuning coefficient: about 2 GHz/K). The laser driver is equipped with an internal bias-tee allowing for fast (up to 2 MHz) external modulation of the QCL current.

The schematic of the QEPAS setup is shown in Fig. 1. The beam exiting the laser is coupled to a hollow-core waveguide (Opto-Knowledge Systems Inc.) by means of optimized coupling optics, and a final output focuser allows for optimal beam focusing between the 300-μm-spaced QTF prongs and passing through the mR system.

#217183 - $15.00 USD Received 16 Jul 2014; revised 15 Sep 2014; accepted 15 Sep 2014; published 5 Nov 2014

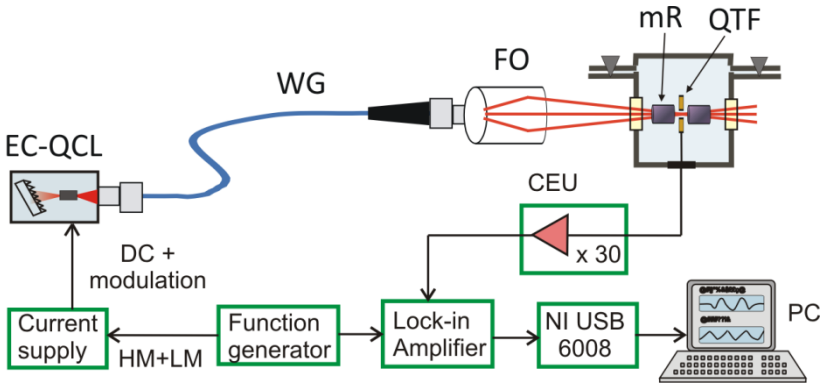

Fig. 1. Schematic of the QEPAS gas sensor. EC-QCL: external cavity quantum cascade laser; WG: waveguide; FO: focusing optics; HM and LM: high-frequency and low-frequency modulation; CEU: control electronic unit; QTF: quartz tuning fork; mR: micro-resonator tubes.

The ADM is housed in a vacuum-tight cell designed for spectroscopic analysis of both static and flowing gas and equipped with two ZnSe windows. The pressure and flow rate of the sample gas through the cell are controlled and maintained at the desired level using a pressure controller and gas flow meter (MKS Instruments Type 640). The mR system consists of two metallic tubes with a length of 4.00 mm each and inner diameter of 0.84 mm, acting as acoustic organ-pipe resonators. The laser beam exiting the QEPAS cell passes through a reference gas cell (length 10 cm) filled with pure H_2S (99.5%) at 5.3 mbar. An IR detector (VIGO model PV-8) subsequently collects the radiation. The recorded absorption spectra allow us to monitor the laser frequency scan. A wavelength modulation (WM) detection technique was implemented by applying a sinusoidal modulation to the QCL current (via the driver internal bias-tee) at half of the QTF resonance frequency $f_0/2$ and detecting the QTF response at f_0 (2*f*-QEPAS) by means of a lock-in amplifier. Unless differently specified, the lock-in amplifier was set to a time constant τ = 200 ms and 12 dB/oct filter slope for all QEPAS measurements reported in this work. QEPAS spectral scans over the molecular absorption line were performed by tuning the laser temperature as described above. Before the lock-in amplifier demodulation, the QTF signal is processed by a transimpedance amplifier (gain resistor *R*g = 10MΩ) positioned very close to the QTF + mR system, and a control electronic unit (CEU). The latter provides also the electromechanical parameters of the QTF: its dynamic resistance R, quality factor Q, and resonant frequency f_0. The physical parameters measured for our QTF at 165 mbar using N_2 as gas carrier were Q = 18986, f_0 = 32759.63 Hz and R = 63.8 kΩ. From the measured resistance we extract a QTF thermal noise of 4.6 μV (0.83 Hz detection bandwidth) [8]. The lock-in amplifier is controlled by an USB data acquisition card (National Instruments DAQ-Card USB6008) via a LabVIEW-based software.

3. Single mode mid-IR fiber coupling system

The HWG used here is similar to that described in [19]. It is realized with an inner silver–silver iodine (Ag–AgI) reflecting coating and has an internal bore size d = 200 μm (~25 times larger than the operating laser wavelength), and a length of 15 cm. To provide single mode transmission it is crucial to optimize the coupling between the laser and the waveguide modes [26]. The fundamental waveguided modes are hybrid HE_{nm}, where HE_{11} is the lowest order mode having a circularly-symmetric Gaussian-like spatial beam profile. Essentially, coupling coefficients for the various modes are governed by the degree to which the focused beam "fills" the hollow bore. Optimal coupling into the lowest order HE_{11} mode occurs for $2w_o/d$ ~0.64, where w_o is the $1/e^2$ radius for a Gaussian beam ($I \propto e^{-2r^2/w_o^2}$) at the waveguide entrance [26, 27]. For a fiber with a bore diameter d = 200 μm, optimal coupling occurs for

#217183 - $15.00 USD Received 16 Jul 2014; revised 15 Sep 2014; accepted 15 Sep 2014; published 5 Nov 2014

w_o = 64 μm, which for λ = 7 μm equates to a numerical aperture $NA = \lambda/(\pi \cdot w_o)$ = 0.035. Thus, relatively slow optics provide optimal coupling into the lowest order mode. When faster optics are used (i.e, giving a laser beam diameter at the waveguide entrance smaller than the core size, so realizing an "under filling condition") there will be less coupling into the lowest order mode and more coupling into the higher order modes. On the opposite extreme, for the case where the beam size is bigger than the bore, the coupling efficiency will naturally go down due to clipping of the beam; however, the lowest order mode will be preferentially exited. Based on this considerations, we designed and realized an optimized laser optical coupling system. It has been fixed directly on the laser mount, thus minimizing mechanical relative vibrations or misalignments of the laser beam. In Fig. 2 the two-dimensional intensity distributions of the laser beam exiting the EC-QCL (Fig. 2(a)) and at ~2 cm away from the HWG exit (Fig. 2(b)) are shown, measured by a pyroelectric infrared camera (Ophir-Spiricon Pyrocam-III). The partially astigmatic beam exiting the laser is cleaned into a good TEM_{00}-like mode at the end of the ~15 cm long fiber, so to be efficiently focused into the QTF + mR module. Moreover, laser tuning does not affect the beam mode exiting the fiber. Propagation losses of 1.34 dB have been determined by measuring the optical power both at the waveguide entrance and at the output of the fiber. We extracted an output-beam divergence of 24 mrad by adopting the approach described in [28]. Note that the beam divergence critically depends on the nature of the optical mode propagating through the guide, the propagating light wavelength and the HWG bore diameter. By using a coupling lens with a nominal focal length of f = 40 mm we estimated, for a Gaussian laser beam, $w_0 = \frac{w}{\sqrt{1+\left(\frac{\pi w^2}{\lambda R}\right)^2}}$ ~68 μm, where R is the radius of curvature of the lens and $2w$ = 2.6 mm is the laser beam diameter, which corresponds to $2w_o/d$ ~0.68, very similar to the optimum value (0.64) for single mode emission. The fiber output focuser was designed and realized in order to provide a focusing distance of 40 mm and produce a laser beam shaping so that the light can be transmitted through the ADM system without hitting it. In Fig. 2(c) the 3D laser beam profile is shown as measured by the pyroelectric camera at the focusing plane of the collimator. From a Gaussian fit of the focused beam profile, shown in Fig. 2(d), we calculated a beam waist diameter of ~170 μm, well below the gap between the QTF prongs (~300 μm). As a result, more than 96% of the laser beam coming out the collimator was transmitted through ADM module without touching it, leading to a barely visible background fringe-like pattern in the QEPAS spectra. Thus, the employment of a HWG in our QEPAS setup provided two main advantages: it avoids optical misalignment when tuning the laser and, at the same time, allows to operate with a mid-infrared excitation beam of high quality and stability. The only minor drawback is a power reduction of about 30% due to the HWG losses and to the uncoated coupling and focusing optics used. Starting from 77 mW exiting the EC-QCL on the peak of the selected absorption line, we measured 53 mW after the focuser. This power attenuation can be further reduced by adopting proper anti-reflection coatings on the optics.

#217183 - $15.00 USD Received 16 Jul 2014; revised 15 Sep 2014; accepted 15 Sep 2014; published 5 Nov 2014

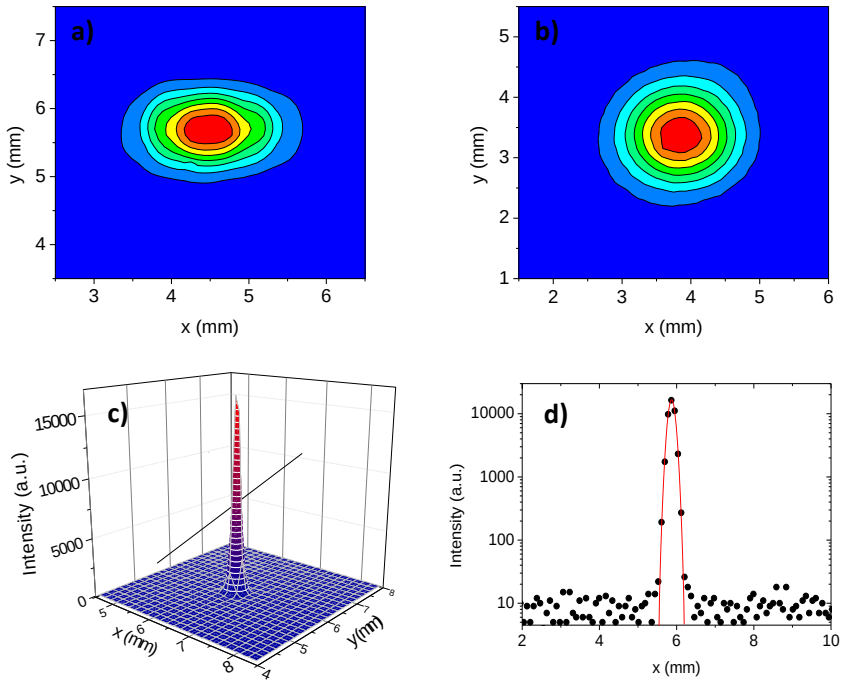

Fig. 2. Two-dimensional intensity distribution of the laser beam exiting the EC-QCL (a) and the HWG (b) measured by a pyroelectric infrared camera. Three-dimensional laser beam profile (c) and one-dimensional profile on a log scale (d) measured by the pyroelectric camera at the focusing plane of the collimator. Solid curve is the best Gaussian fit of the focused-beam profile.

4. H_2S trace-gas detection

A crucial issue for H_2S field measurements is to avoid interference effects from H_2O, since the presence of water vapor can strongly affect or even destroy the performances of H_2S sensors, while gas sensing in a range free from strong water absorption allows gaining in sensitivity and reproducibility. In Fig. 3 we show the simulated absorption spectra for a gas mixture of standard air and 10 ppm of H_2S at 160 mbar pressure in the range 1266.8-1267.0 cm^{-1}, using HITRAN database. For the sensor validation we selected the H_2S absorption line falling at 1266.933 cm^{-1} and belonging to the (010-000) vibrational band, with a linestrength $S = 1.51 \cdot 10^{-21}$ cm/mol (HITRAN units [29]). We chose this line also because it is one of the strongest available for H_2S in the EC-QCL operating range. At ~1266.883 cm^{-1} an absorption line due to water vapor is clearly visible but, at the selected gas pressure, it doesn't sensibly affect the H_2S peak absorption.

#217183 - $15.00 USD Received 16 Jul 2014; revised 15 Sep 2014; accepted 15 Sep 2014; published 5 Nov 2014

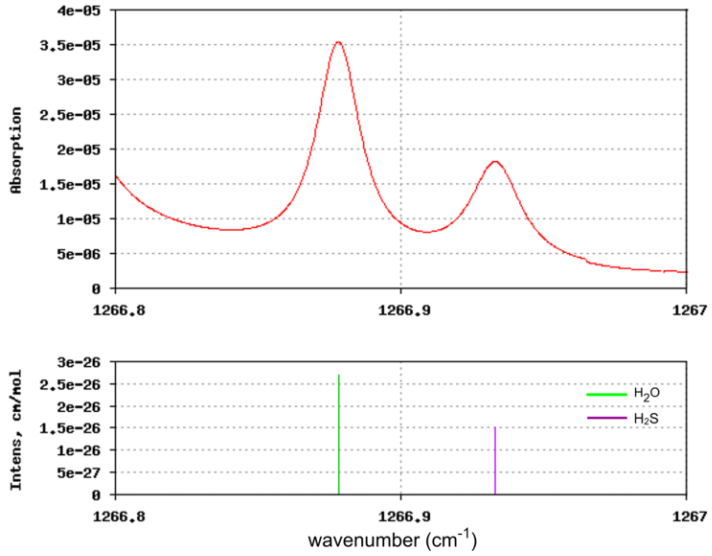

Fig. 3. Simulation of direct absorption spectrum of a gas sample composed by 10 ppm H_2S in N_2 with 2% water vapor. The sample pressure has been set to 160 mbar, the same as used in our setup. The absorption path has been (arbitrarily) set to 10 cm. At the working pressure the water lines do not sensibly affect the H_2S peak absorption, limiting their interfering effect to the tails of the line profile.

To find the optimal operating condition in terms of QEPAS signal-to-noise ratio, we investigated the effects of gas pressure and WM amplitude. Figure 4 shows the obtained results for a gas mixture composed of 120 ppm H_2S in N_2. The optimal sensor operating conditions were found to occur at a gas pressure of 160 mbar (Fig. 4(a)) and a modulation amplitude $\Delta\lambda$ of 10 V peak-to-peak (Fig. 4(b)), limited by the modulation capability of our waveform generator and corresponding to about 0.03 cm^{-1} modulation depth.

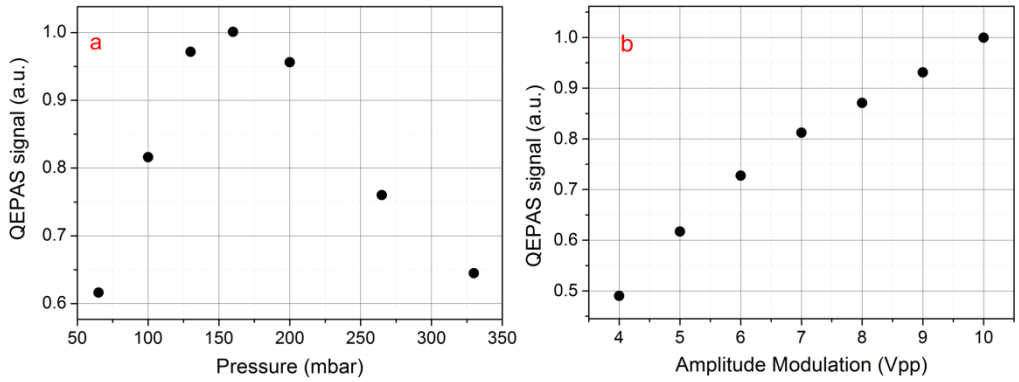

Fig. 4. (a) Normalized QEPAS peak signal as a function of sample pressure: we selected 160 mbar as optimal sample pressure. (b) Normalized QEPAS signal amplitude plotted at 160 mbar as a function of the QCL modulation voltage (conversion coefficient: about 0.003 cm^{-1}/V). Both data sets were measured for 120 ppm H_2S concentration in N_2.

We used a trace gas standard generator used to produce H_2S concentrations in the range 0-500 ppm, employing pure or humidified N_2 as the diluting gas, starting from a certified 500 ppm H_2S in N_2 mixture. Several 2*f*-QEPAS spectral scan acquisitions have been obtained for different H_2S concentrations and the related measured QEPAS peak values are reported in Fig. 5. A linear fit of the data demonstrates the good linearity of the sensor versus H_2S concentration.

#217183 - $15.00 USD Received 16 Jul 2014; revised 15 Sep 2014; accepted 15 Sep 2014; published 5 Nov 2014

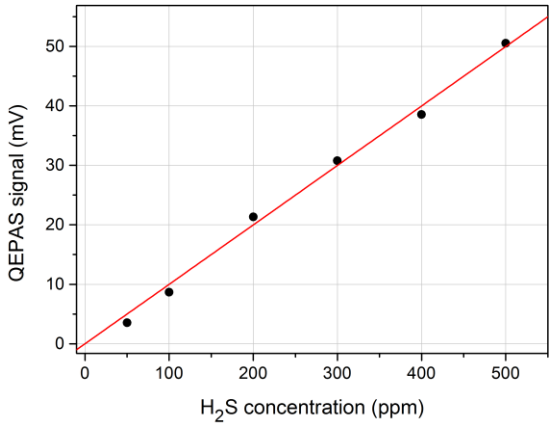

Fig. 5. QEPAS signal (2*f* detection) as a function of H_2S concentration: the linear fit (solid line) shows the linearity of the sensor. The intercept is forced to zero and the adjusted R-square results 0.998.

A representative *2f*-QEPAS spectral scan of a 100 ppm H_2S:N_2 gas mixture sample is shown in Fig. 6(a). The spectrum has a typical second-derivative shape, slightly distorted because of non-negligible residual amplitude modulation of the QCL during the scan [15]. The spectrum has been acquired with the lock-in amplifier set to 200 ms integration time and 12 dB/oct filter slope. By analyzing the signal-to-noise ratios (S/N) of all the acquired spectra, we extracted a minimum detectable concentration (at S/N = 1) C_{min} = 3 ppm of H_2S in dry N_2. The measurements have been repeated also for humidified N_2 (up to 2% water vapor concentration), and no significant variations of the signal-to-noise ratio have been recorded. This verifies two assumptions. In terms of gas mixture excitation, the water absorption lines are far enough from the selected H_2S one in order not to influence, at the selected working pressure, the QEPAS signal. As for what the de-excitation processes are concerned, H_2O does not act as a relaxation promoter for the gas mixture. This can be expected since H_2S shows fast vibrational de-excitation velocity, similar to that of H_2O [30]. As a consequence, in-field operation of our sensor would not require any water concentration calibration. It is finally worth noting that the time duration of a single scan is much longer than the integration time but, as the 2*f*-QEPAS signal is background free, once the sensor has been calibrated it is sufficient to measure the peak value by acquiring a single point to retrieve the sample concentration. Thus our QEPAS sensor can work in real time with a time response below 1s.

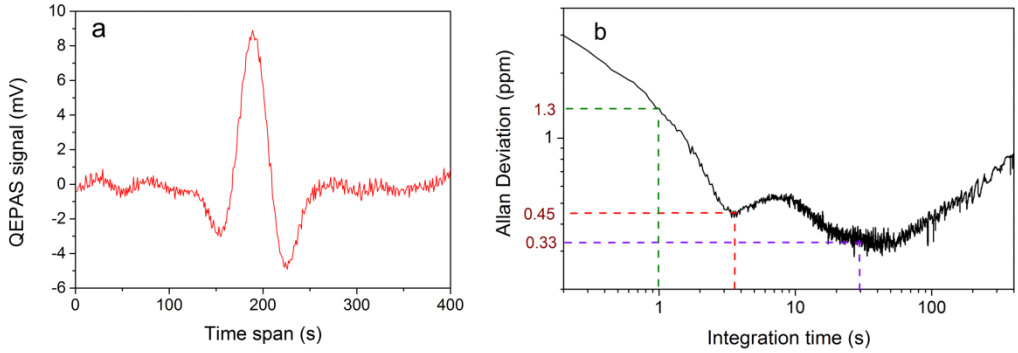

Fig. 6. (a) Spectral scan of a 100 ppm H_2S:N_2 sample at 160 mbar and with 200 ms integration time. (b) Allan deviation of the I-QEPAS signal as a function of the integration time. The curve has been calculated by analyzing a 100 minutes-long acquisition of the signal (150 ms sampling time and lock-in amplifier set to 50 ms time constant) measured in locking conditions for pure N_2 at 160 mbar pressure.

#217183 - $15.00 USD Received 16 Jul 2014; revised 15 Sep 2014; accepted 15 Sep 2014; published 5 Nov 2014

In order to determine the best achievable sensitivity of the QEPAS sensor we performed an Allan deviation analysis, measuring and averaging the QEPAS signal for pure N_2 at 160 mbar pressure under the optimized QEPAS operating conditions. As shown in Fig. 6(b), for a 1 s integration time a C_{min} = 1.3 ppm is reached, which, for averaging times of 3.5 s, drops down to 450 ppb, a record value for H_2S optical detection. The latter corresponds to a minimum absorption coefficient $\alpha_{min} = 3.5 \cdot 10^{-8}$ cm^{-1}. By taking into account the laser power available for sample interaction (~45 mW due to partial reflection by the ZnSe entrance window of the vacuum-thigh cell), we extract a NNEA of $7.3 \cdot 10^{-9}$ $Wcm^{-1}Hz^{-1/2}$.

5. Conclusion

In this work we have reported on a widely-tunable QEPAS spectrometer operating around 8 μm wavelength based on a single-mode fiber-coupled EC-QCL. The HWG allows to clean the astigmatic beam exiting the QCL into a TEM_{00}-like mode, optimal for beam focusing through the QTF. Moreover, the use of a hollow-core fiber allows to fully exploit the wide tunability of the laser source, avoiding any optical misalignment with the ADM module produced by mechanical rotations of the external-cavity grating. Spectroscopic validation of the sensor has been carried out selecting as target gas H_2S, a toxic molecule of crucial importance for petrochemical and environmental monitoring applications. Background-free spectral scans for different H_2S concentrations have been performed in order to verify the sensor linearity. The sensor allows for rapid measurements (200 ms integration time) down to a detection limit of 3 ppm of H_2S in N_2. The sensitivity can be improved by about one order of magnitude (330 ppb) by increasing the integration time up to ~30 seconds. Noteworthy, at the operating pressure of 160 mbar the selected absorption H_2S line is not sensibly affected by the presence of water vapors (up to few %) in the gas mixture and make our sensor usable for in field on-line H_2S measurements.

Acknowledgments

The authors from CNR-INO gratefully acknowledge the financial support from Regione Toscana, within the frame of POR CReO FESR 2007-2013, Project SIMPAS (Innovative Measurement Systems for the Protection of Environment and Health). The authors from Dipartimento Interateneo di Fisica di Bari acknowledge financial support from three Italian research projects: PON01 02238, PON02 00675 and PON02 00576.

#217183 - $15.00 USD Received 16 Jul 2014; revised 15 Sep 2014; accepted 15 Sep 2014; published 5 Nov 2014